Contents

1 Introduction 4

2 Theory 10

3 Results and discussions 16

4 Conclusions 35

List of Figures

1.1 A schematic illustration of the proposed spin-filter device. The channel length on the InAs layer is 200nm along the z axis, the distance between the two gates is 100nm, and the in-plane wave vector is parallel to the y axis. 8

1.2 A symmetric resonant barrier induced by the double gates is along the z axis and extended to 200nm. 9

2.1 The barrier with an external electric field adding is 200 nm long. ΔV is the voltage drop. 15

3.1 Tunneling transmission probability based on logarithm scale varies with energy. ($k_y = 0\, m^{-1}$) 21

3.2 Tunneling transmission probability based on logarithm scale is energy dependent. ($k_y = 0.5 \times 10^8\, m^{-1}$) 22

3.3 Tunneling transmission probability based on logarithm scale depends on electron energy. ($k_y = 1 \times 10^8\, m^{-1}$) 23

3.4 Spin polarization depends on spin-orbit interaction parameter linearly at zero temperature and voltage drop($0.00137\, V$) based on the two doping concentrations. ($n_{F1} = 1.93 \times 10^{11} cm^{-2}$, $n_{F2} = 2.42 \times 10^{11} cm^{-2}$) 24

3.5 Spin polarization is a function of the external electric field, F_z ,under three different spin-orbit interaction parameters.($n_F = 1.93 \times 10^{11} cm^{-2}$, $T = 0\,K$) 25
3.6 Spin polarization depends on temperature based on three different bias values.($n_F = 1.72 \times 10^{11}\,cm^{-2}$, $\alpha = 1.5 \times 10^{-11}\,eV \cdot m$) 26
3.7 J_+ represents spin-up current, and J_- represents spin-down current. And the bias points(A and B) mean the different energy states appear or disappear.($n_F = 1.93 \times 10^{11}\,cm^{-2}$,$\alpha = 1.5 \times 10^{-11}\,eV \cdot m$,$T = 0\,K$) 27
3.8 The distance between the centers of the double gates is shorten to 40 nm, and ΔV represents the voltage drop. 28
3.9 The first energy state in the short barrier have been lifted up to 0.018eV. 29
3.10 Spin polarization remains 100% in a low temperature region and decays fast as the temperature increasing.($n_F = 1.72 \times 10^{11} cm^{-2}$, $\alpha = 1.5 \times 10^{-11}\,eV \cdot m$) 30
3.11 100% polarization remains in a short bias region.($n_F = 1.72 \times 10^{11} cm^{-2}$,$\alpha = 1.5 \times 10^{-11}\,eV \cdot m, T = 0\,K$) 31
3.12 The current is only for a spin-down current and nearly linear with the external electric field in the low bias region at zero temperature.($n_F = 1.72 \times 10^{11}\,cm^{-2}$,$\alpha = 1.5 \times 10^{-11}\,eV \cdot m$) . 32
3.13 The two barriers induced by the mismatch gates along the z axis have different heights(0.1V and 0.2V) and half width(17nm, 9nm). 33
3.14 The tunneling transmission probability based on logarithm scale is calculated from the asymmetric barrier, and there are still energy states here. 34

Chapter 1

Introduction

Spin-orbit interaction on the 2D electron gas system with zero magnetic field has drawn significant interest. It's proved that the polarization of electrons can be manipulated via the applied gate voltage which can alter spin orbit interaction originating from the lack of inversion symmetry in macroscopic confining potential called Rashba term. The discussion on such a phenomena on an electronic device based on semiconductor was pushed forward by Datta and Das in 1990[1]. The source and drain are both ferromagnetic metals with the same alignment of electron spin. Electrons will be injected into the source which will align the spin orientation of the electrons the same way as those in the source. Besides,resonant double-barrier tunneling structures have attracted considerable attention since the pioneering work of Tsu and Esaki[2]. But almost all theoretical calculations are done by one-dimensional approach for determining tunneling transmission probability. Recently a few papers have called attention to some peculiarities in the dependence of the tunneling transmission probability on the parallel electron wave-vector for symmetric tunnel hetrostructures[3, 4, 5]. It was found that for structures with an electronic effective mass dependent on space position, and the in-

plane wave-vector can be the key point in the transmission process.

The charge degree of freedom of electrons is a key point to the success of semiconductor electronics. The spin degree of freedom had always been neglected in semiconductors largely due to the almost degenerate energies of two spin states of electrons. But, with the improvement of semiconductor process, the working dimension of semiconductor electronic devices has been reduced to a nano-scale, so spin-orbit interaction among electrons has to be taken into consideration. As time past, there has been a rapid development of semiconductor spin devices. In general, spintronics includes not only semiconductor materials but many other systems. However, it could leads to a widespread application only cooperating with modern semiconductor technology. Moreover, spin degree of freedom is perhaps more advantageous than charge because unlike charge spin is not coupled to electromagnetic noise and therefore has much longer coherent time[6]. Furthermore, adding spin degree of freedom to conventional charge-based electronic devices has the potential advantages of non-volatility, increased data processing speed, and decreased electric power consumption.

The utilization of the spin-orbit interaction has played the main role on semiconductor spintronics. However, there are some challenges existing in semiconductor technology, like efficient injection, transport control, manipulation, and detection of spin polarization. A natural starting point to tackle those problems would be to pass electrons through strongly magnetized metals and then inject them back to semiconductor. But the conductivity mismatch between metal and semiconductor impedes the electron transport and makes this approach seem inefficient, as Schmidt pointed out[20]. And a most elementary issue, an efficient means to obtain spin polarized currents in semiconductor structures, has not been resolved yet. The inefficiency of

spin-injection back from magnetized metal electrodes sparks interest in all semiconductor alternatives. The spin-orbit interaction of electrons in III-V semiconductor junctions, which thus provides a possible way. The spin-orbit interaction in III-V semiconductor materials is usually described by two contributions to the effective one-band spin dependent Hamiltonian. One is the Rashba term induced by the inversion asymmtry of the macroscopic potential, which can be controlled by an external electric field or material growth techniques. The other is the Dresselhaus term[21] due to the inversion asymmetry of the zinc-blende lattice. The interplay between these two terms has been studied by de Andrada Silva[21], showing that, for narrow gap semiconductors, the contribution from the Rashba term to the spin- orbit interaction dominates over that from the Dresselhaus term.

The spin-orbit interaction in semiconductor hetrostructures can be caused by an electric field perpendicular to the two-dimensional electron gas system. Riding on an electron, this electric field will be felt as an effective magnetic field lying in the plane of the 2DEG, perpendicular to wave vector k of the electron. The effective Zeeman interaction of the electron spin with the field lifts the spin degeneracy(internal Zeeman effect). This is usually referred to in the literature as the Bychkov-Rashba mechanism. This results in an isotropic spin splitting energy Δ_{so} at B=0 proportional to k[7]. For electrons moving along the shortest way from the source to drain, the energies of the two spin states are

$$E_{\pm} = \frac{\hbar^2 k^2}{2m^*} \pm \alpha k. \tag{1.1}$$

α is a material dependent coefficient which can be altered by the external electric field. For a given Fermi energy E_F there are two wave vectors k_+ and k_- corresponding to the solution of the equation $E_{\pm} = E_F$. The Fermi level is a pair of concentric circles with radii k_+ and k_-. Experimentally observed

values of the spin orbit coupling strength α lie in the range of $0.5 \sim 4.5$ $10^{-11} eV \cdot m$[8, 9]. Calculation based on the Rashba spin-orbit interaction in III-V semiconductor heterostructures have been performed[10, 11, 12, 13, 14, 15], showing the entire semiconductor tunneling structures can be a feasible means to obtain electronic spin-polarized currents.

In this report, we propose a device made of GaAS/InAs/GaAs shown in Fig. 1.1. The channel is along the z axis, and there is a double symmetric potential barrier shown in Fig. 1.2 induced by the double metallic gates which is used to form the confining barrier, and the wave vector in y direction is continuous. When an electron is injected into the source, it will be accelerated by the voltage drop across the source and drain. But it wouldn't always arrive at the drain because of the double barrier. In Eq. (1.1), we can demonstrate that any two electrons with opposite spin-orbit orientations will be in different energies even with the same wave vector if we take the spin orbit interaction into consideration. That's the reason why we can get spin polarized current. Furthermore, we could get a recognizable magnitude of polarization with the well defined potential barrier and Fermi energy.

This report is organized as follows: in chapter 2, we present the essential formalism for our study and the numerical approach we use to calculate the tunneling transmission probability. The calculation results and discussions are shown in chapter 3. Finally, we summarize our work in chapter 4.

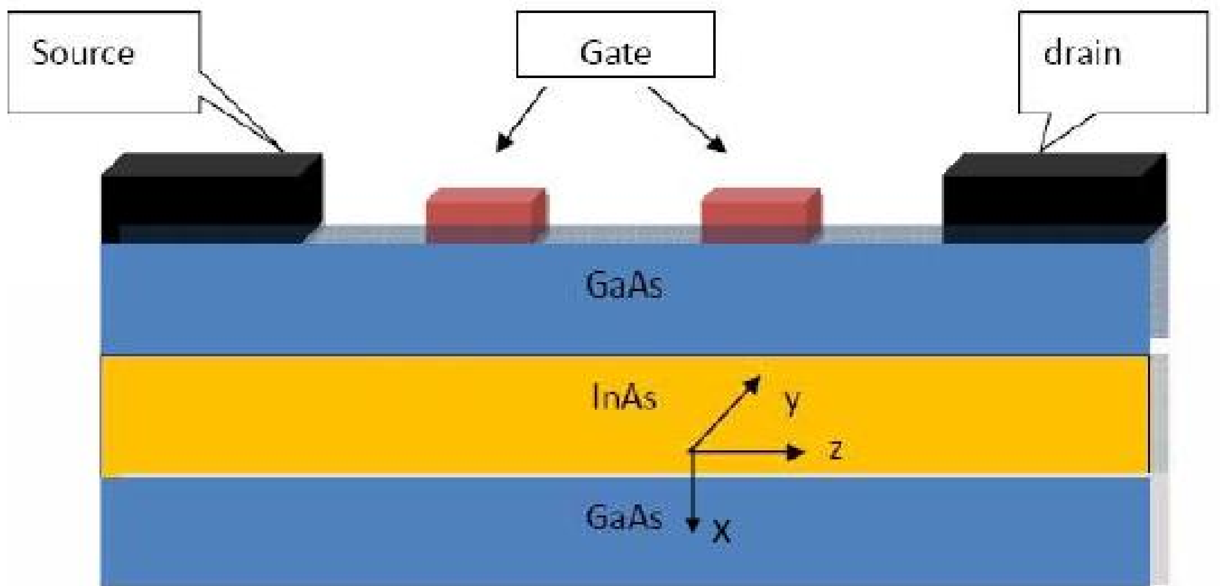

Figure 1.1: A schematic illustration of the proposed spin-filter device. The channel length on the InAs layer is 200nm along the z axis, the distance between the two gates is 100nm, and the in-plane wave vector is parallel to the y axis.

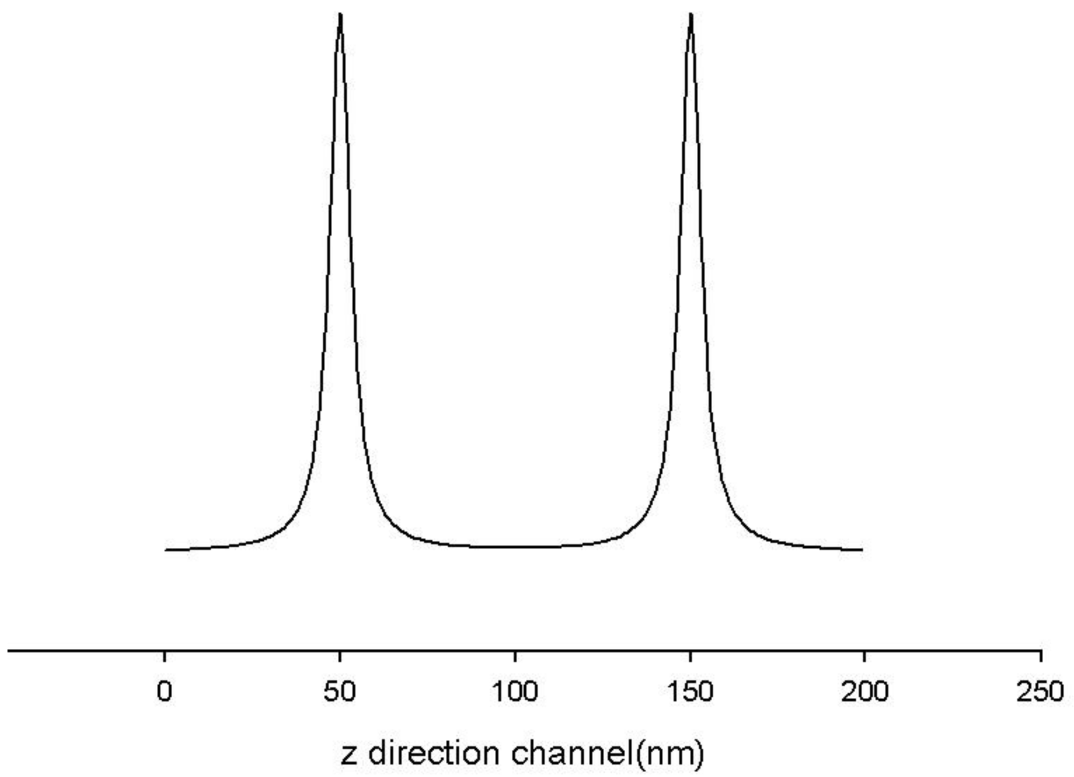

Figure 1.2: A symmetric resonant barrier induced by the double gates is along the z axis and extended to 200nm.

Chapter 2

Theory

We have investigated the spin-dependent tunneling process through a spin filtering system shown in Fig. 1.1. This is a two dimensional electron gas system. There the double metallic gates will induce a double potential barrier on the InAs channel between the source and drain, and the barrier with a voltage drop is shown in Fig. 2.1. In x direction, there is a traditional quantum well based on GaAs/InAs/GaAs, so we could take Rashba spin orbit interaction into consideration in the tunneling process under nonzero average electric filed providing by the double gates. The electron motion direction is on y-z plane, and the in-plane wave vector is denoted by k_y.

Our calculation is performed in the base of the effective electronic one band Halmiltonian[10, 11], energy- and position- dependent electron effective mass approximation, the Ben Daniel-Dike boundary conditions[20], and the multi-step approximation[17] with cutting the barrier into a sequence of N small segments. On the basis of the above assumptions the electronic wave function[16] in the lth segment can be interpreted as

$$\Phi_l(z, y) = \Psi_l(z) \exp(ik_y \cdot y), \qquad (2.1)$$

where $\Psi_l(z)$ satisfies the z-component of the Schrödinger equation

$$\hat{H}_l \Psi_l(z) = E\Psi_l(z), \tag{2.2}$$

with the spin-dependent Halmiltonian in each region[22]

$$\hat{H}_l = \hat{H}_{l0} + \hat{H}_{lso}. \tag{2.3}$$

Where $\hat{H}_{l0}$ is the Hamiltonian of the system without spin-orbit interaction

$$\hat{H}_{l0} = -\frac{\hbar^2}{2}\frac{\partial}{\partial z}\frac{1}{m_l(E)}\frac{\partial}{\partial z} + \frac{\hbar^2 k_y^2}{2m_l(E)} + E_c + eV(z), \tag{2.4}$$

and

$$\frac{1}{m_l(E)} = \frac{P^2}{\hbar^2}\left[\frac{2}{E - E_c + E_g + eV_l} + \frac{1}{E - E_c + E_g + \Delta + eV_l}\right], \tag{2.5}$$

presents the energy and position dependent reciprocal effective mass. E denotes electron energy in the conduction band, and V_l is the double barrier potential function induced by the double metallic electrodes in lth region. The momentum matrix element P does not rely on z,[16] and E_c, E_g and Δ stand for the corresponding the bottom of conduction-band, the band gap, and the spin-orbit splitting in the valence band, and e is an absolute value of an electron charge. When the kinetic energy of electrons is substantially smaller than the barrier's height we can present this term as the following

$$\hat{H}_{lso} = \alpha(\sigma_z \hat{k_y} - \sigma_y \hat{k_z}), \tag{2.6}$$

where σ_z and σ_y are correspondingly z and y components of the vector of the Pauli matrices $\hat{\sigma} = \{\sigma_x\,, \sigma_y\,, \sigma_z\}$ and α is a material dependent constant.

The boundary conditions for the solution $\Psi_l(z)$ at the interface between l and $l+1$ regions have been introduced in Ref.[16]

$$\frac{1}{m_l(E)}\left\{\frac{d}{dz}\Psi_l(z)\right\}_{z=z_l} = \frac{1}{m_{l+1}(E)}\left\{\frac{d}{dz}\Psi_{l+1}(z)\right\}_{z=z_l},$$

$$\Psi_l(z_l) = \Psi_{l+1}(z_l).$$

$$\Psi_l(z) = A_l(z)\exp(ik_{zl}z) + B_l(z)\exp(-ik_{zl}z). \tag{2.7}$$

The above is the general solution of Eq. (2.2) in the lth region. And $\exp(\pm\, i\, k_{zl}\, z)$ is a pair of linear independent solutions of Eq. (2.2) within that region. Inside the linear independent solutions

$$k_{zl} = \frac{\sqrt{2m_l(E)(E - U_l(E,k_y))]}}{\hbar}. \tag{2.8}$$

$$U_l(E,k_y) = \frac{\hbar^2 k_y^2}{2m_l(E)} + E_c + V_l,$$

where V is the confining potential,

$$V_l = V\left(\frac{z_{l-1}+z_l}{2}\right),$$

and m is energy and position dependent effective mass,

$$m_l(E) = m\left(E, \frac{z_{l-1}+z_l}{2}\right),$$

and

$$S_l(E,k_y) = \frac{m_{l+1}(E)}{m_l(E)}\frac{k_{zl}(E,k_y)}{k_{z_{l+1}}(E,k_y)}.$$

The coefficients $\{A_l(z), B_l(z)\}$ are to be determined from the boundary conditions, Eq. (2.7). The sets of coefficient in neighboring regions are related by the transfer matrix M[23]:

$$\begin{pmatrix} A_l \\ B_l \end{pmatrix} = M_l \begin{pmatrix} A_{l+1} \\ B_{l+1} \end{pmatrix}$$

$$M = \begin{pmatrix} M_{11} & M_{12} \\ M_{21} & M_{22} \end{pmatrix} = \prod_{l=0}^{N} M_l, \tag{2.9}$$

where

$$M_l = \frac{1}{2} \left(\begin{array}{l} (1+S_l(E,k_y)) \exp[-i(k_{z_{l+1}}(E,k_y) - k_{z_l}(E,k_y))z_l] \\ (1-S_l(E,k_y)) \exp[i(k_{z_{l+1}}(E,k_y) + k_{z_l}(E,k_y))z_l] \end{array} \right.$$

$$\left. \begin{array}{l} (1-S_l(E,k_y)) \exp[-i(k_{z_{l+1}}(E,k_y) + k_{z_l}(E,k_y))z_l] \\ (1+S_l(E,k_y)) \exp[i(k_{z_{l+1}}(E,k_y) - k_{z_l}(E,k_y))z_l] \end{array} \right). \tag{2.10}$$

Moreover, we calculate the tunneling transmission probability and the spin polarized currents as following

$$T(E,k_y) = \frac{m_0(E)}{m_{N+1}(E)} \frac{k_{zN+1}(E,k_y)}{k_{z0}(E,k_y)} |A_{N+1}|^2, \tag{2.11}$$

where

$$A_{N+1} = \frac{m_{N+1}(E)}{m_0(E)} + \frac{k_{z_0}(E,k_y)}{k_{zN+1}(E,k_y)} \frac{1}{M_{22}},$$

where M_{22} is a factor of the transfer matrix M in Eq. (2.9).

The total electron energy with the consideration of the spin-orbit interaction, E can be regarded as

$$E = E_c + \frac{\hbar^2(k_y^2 + k_z^2)}{2m(E,z)} + \sigma\,\alpha\,\sqrt{k_y^2 + k_z^2}, \tag{2.12}$$

where $\sigma = \pm 1$ refers to spin polarization, α denotes the Bychkov-Rashba spin-orbit interaction parameter, and we set the bottom of the conduction band as a reference, $0\ eV$. Next, we calculate spin polarized currents as follows:[13] the total current is

$$J = J_+ + J_-,$$

$$J_\sigma = \frac{e}{2\pi^2}\int_0^\infty dk_z \int_0^\infty dk_y\, T(E,k_y)[f_{source(k_y,k_z)-f_{drain}(k_y,k_z)}]u_{z_\sigma}, \tag{2.13}$$

where e is an absolute value of an electron charge. f_{source} and f_{drain} are the electron distribution functions represented as following

$$f_{source}(k_y,k_z) = \frac{1}{\exp(\frac{E-E_F}{k_BT})+1},$$

$$f_{drain}(k_y,k_z) = \frac{1}{\exp(\frac{E-E_F-\Delta V}{k_BT})+1}.$$

$f_{source}(k_y,k_z)$ and $f_{drain}(k_y,k_z)$ are presented by Fermi-Dirac distribution. E_F denotes the Fermi energy and could be controlled by the doping concentration n_F, ΔV is the voltage drop between the source and drain controlled by the external electric field F_z, and u_{z_σ} is the longitudinal velocity depending on the spin-orbit orientations[7] in the source and can be written as

$$u_{z_\sigma} = \frac{1}{\hbar}\frac{\partial E}{\partial k_z}. \tag{2.14}$$

Finally, the polarization is defined as

$$P = \frac{J_+ - J_-}{J_+ + J_-}. \tag{2.15}$$

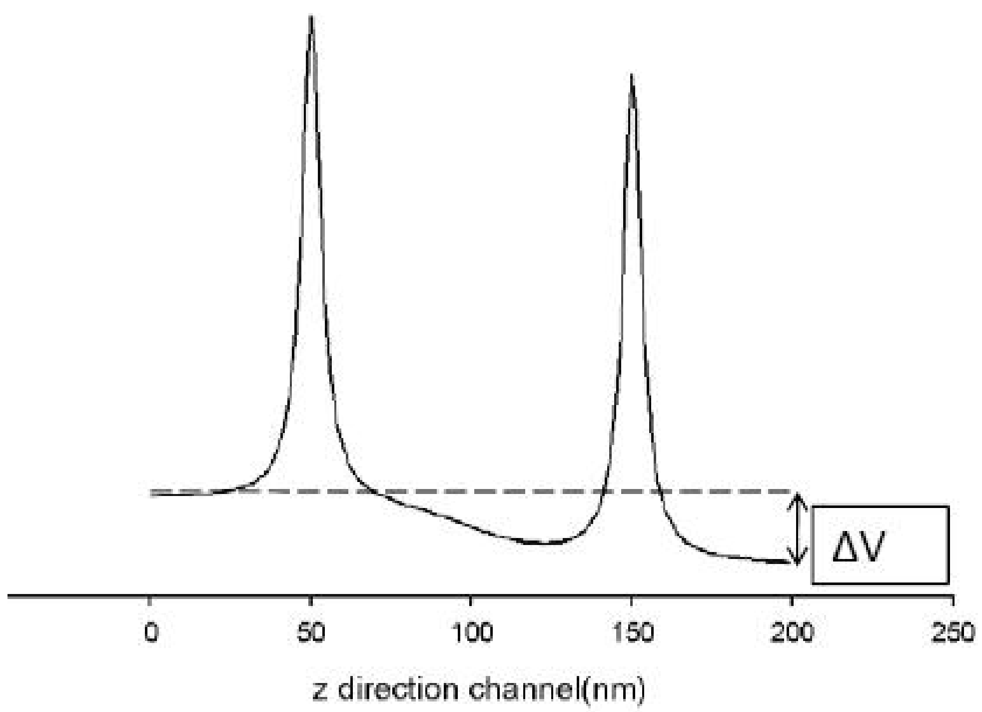

Figure 2.1: The barrier with an external electric field adding is 200 nm long. ΔV is the voltage drop.

Chapter 3

Results and discussions

The tunneling transmission probability is a function of electron energy and in-plane wave vector k_y, and shown in Figs. (3.1, 3.2 and 3.3) calculated by Eq. (2.11). Here we suppose $E_c = 0\ eV$, and the other parameters are obtained from Refs.19: $E_g = 0.42\ eV$, $\Delta = 0.38\ eV$, $m = 0.023m_0$ (m_0 is a free electron mass.). Based on the above results, we could demonstrate that the double potential barrier could be regarded as a bowl shape resonant quantum well. Therefore every peak could be interpreted as a quantum state, and the in-plane wave vector, k_y, is just to lift up the energy level. From our assumption, we could get equations as follows:

$$\frac{\hbar^2(k_z^2 + k_{y_0}^2)}{2m^*} = E_{10}$$
$$\frac{\hbar^2(k_z^2 + k_{y_1}^2)}{2m^*} = E_{11}$$
$$\frac{\hbar^2(k_z^2 + k_{y_2}^2)}{2m^*} = E_{12}\ . \tag{3.1}$$

There we assign $k_{y_0} = 0\ m^{-1}$, $k_{y_1} = 0.5 \times 10^8\ m^{-1}$, $k_{y_2} = 1 \times 10^8\ m^{-1}$, $E_{10} = 0.0034eV$, $E_{11} = 0.0075eV$, and$E_{12} = 0.0198eV$ according to Figs.(3.1, 3.2 and 3.3), so we solve any two equations among Eq. (3.1) and get roughly

$m^* = 0.023m_0$ and $k_{z1} = 4.55 \times 10^7 m^{-1}$. With a microscopic point of view, the effective mass is energy and space dependent, but we could suppose an equivalent mass in the tunneling process with a macroscopic point of view and get discrete longitudinal wave vectors, k_z. As a result, only certain electrons which match the energy levels with longitudinal energy could tunnel through the potential barrier no matter the in-plane wave vector, k_y. In addition, in the presence of spin-orbit interaction originating from the structure inversion asymmetry controlled by the double gates electrons with opposite spin orbit orientation will be in different energies because of non-parabolic dispersion relation, and that is the reason why there exists spin polarized currents. And the spin polarization is not meaningless because of the difference between these two currents(J_+,J_-) in Eq. (2.13). Moreover, we will demonstrate what have influences on the spin polarization in Figs. (3.4, 3.5 and 3.6). From the above results, it can be clarified that spin polarization is linear with the external electric field F_z and the Rashba spin-orbit interaction parameter α shown in Eqs. (2.13) and (2.15). In addition we can get different straight lines with setting different Fermi levels in Fig. 3.4 and the lower Fermi level the higher polarization. As we can see, the quantum effect is more apparent in the low energy region. Moreover, the difference between these two lines(n_{F1},n_{F2}) is proportional to α. Furthermore, in Fig. 3.5 we show the relation between polarization and the external electric field F_z based on different spin-orbit interaction parameters, α. Here we can see spin polarization appears with the external electric field F_z adding. That's because there are three energy states lower than the Fermi level. And even a little electric field is added, there are empty states under the Fermi level E_F in the drain, so some electrons whose longitudinal energies match these three levels will tunnel the barrier immediately, and then spin polarization appears because of the difference

between the different spin polarized currents. In Fig. 3.5, we demonstrate that spin polarization only survive in the low temperature region because a quantum effect is disappeared at high temperatures.

The I-V curve is shown in Fig. 3.7. The current is nearly linear with the external electric field, F_z in the low bias region. Then the first energy state E_1 is disappeared at bias point A because the first energy state continues lowering as the electric field raising. When the first energy state is lower than the lowest energy of the electron in the source, the state will be disappeared. The second energy state E_2 is disappeared at bias B, but the forth state appears at the same time. Consequently, which state appears or not is controlled by the external electric field. That's to say in principle we can control any states we desire in the allowable region with the well defined doping concentration and the external field. Then every energy state under different various bias points are shown in Table 3.1.

Furthermore, we present the next work based on the above idea. If we consider spin-orbit interaction in the source and drain, electrons with opposite spin-orbit orientations will be in different energies. And the lowest longitudinal energy for opposite spin polarized electrons which could tunnel the barrier are $E_{\pm} = \frac{\hbar^2 k_z^2}{2m} \pm \alpha k_z$, where k_z is a discrete longitudinal wave vector parallel to the z axis because of the double barrier on the way to the drain. So, we could control Fermi level and makes

$$E_{-} < E_F < E_{+}. \tag{3.2}$$

Consequently, spin "up" electrons' energies will be never lower than Fermi level and only spin "down" electrons have possibility to tunnel through the barrier. Here we need to shorten the length between the double gates to 40 nm, then the first energy state will be lifted up because $(E_{n+1} - E_n) \propto 1/d^2$

Table 3.1: Energy states depend on various bias points with zero in-plane wave vector.

$F_z(V/m)$	$E_1(eV)$	$E_2(eV)$	$E_3(eV)$	$E_4(eV)$
0	0.0033	0.0094	0.0179	0.0304
6867	0.0027	0.0087	0.0173	0.0297
13734	0.0019	0.008	0.0167	0.0291
20601	0.0012	0.0074	0.0165	0.0284
24721	0.0007	0.007	0.0156	0.02795
27468(A)	X	0.0067	0.0154	0.0263
41202	X	0.0065	0.0152	0.0251
54936	X	0.0042	0.0128	0.0238
75537	X	0.0024	0.0112	0.023
96138	X	0.0006	0.0092	0.0202
109872(B)	X	X	0.008	0.0195
123606	X	X	0.0068	0.018

where d is the distance between the centers of these two gates. And the barrier with bias is shown in Fig. 3.8. The energy level is more reasonable for us to set up the doping concentration. Then the new tunneling transmission probability is shown in Fig. 3.9 based on Eq. (2.11). Consequently, we set up Fermi energy $0.0164eV$, and we get 100% spin polarization shown in Figs. (3.10 and 3.11) based on Eqs. (2.13) and (2.15). One is the relation between spin polarization and temperature, and the other is the relation between the external field and spin polarization. These two plots are both based on the same doping concentration, $n_F = 1.72 \times 10^{11} cm^{-2}$, and Rashba spin-orbit interaction parameter, $\alpha = 1.5 \times 10^{-11}\, eV \cdot m$. The fist one shows that 100% polarization remains in a very low temperature region and very sensitive to the temperature. The second one shows that 100% remains only in a low bias region because the discrete wave vector k_z will be lowering as the external electric field increasing. When E_+ is lower than E_F the spin "up" current appears in Eq. (2.13) and we would lose 100% spin polarization. Furthermore, the I-V curve at zero temperature is shown in Fig. 3.12,and this is only for a spin down current.

Then, we consider the condition about the mismatch of the double gates in advanced. If the barrier is like Fig. 3.13, the tunneling transmission probability in Eq. (2.11) is shown in Fig. 3.14, but the energy states still survive. So, we could calculate the transmission probability, spin polarized currents, and spin polarization in the same way (Eqs. (2.11), (2.13) and (2.15)) and get a recognizable magnitude about 20%. That's to say we can calculate arbitrary shape of potential barrier in principle.

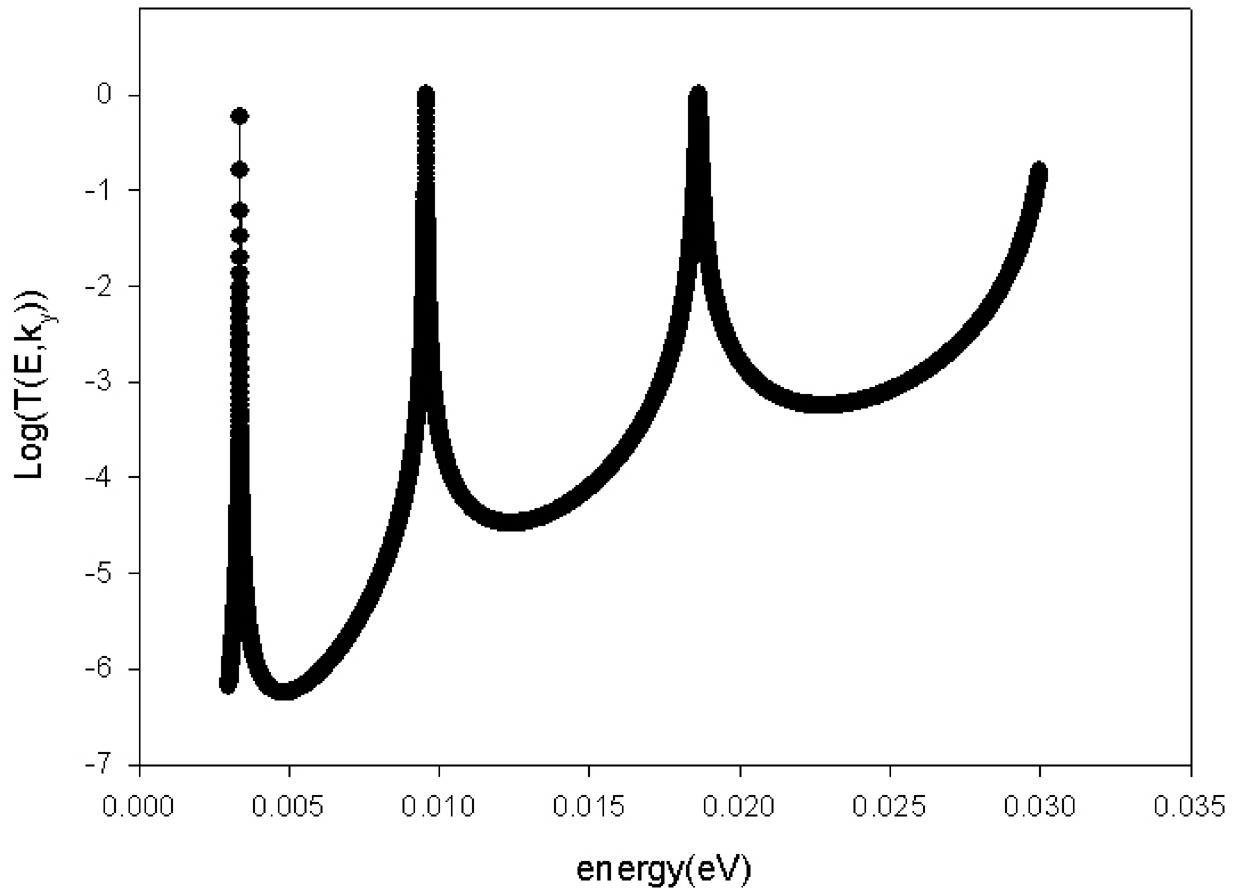

Figure 3.1: Tunneling transmission probability based on logarithm scale varies with energy. ($k_y = 0\, m^{-1}$)

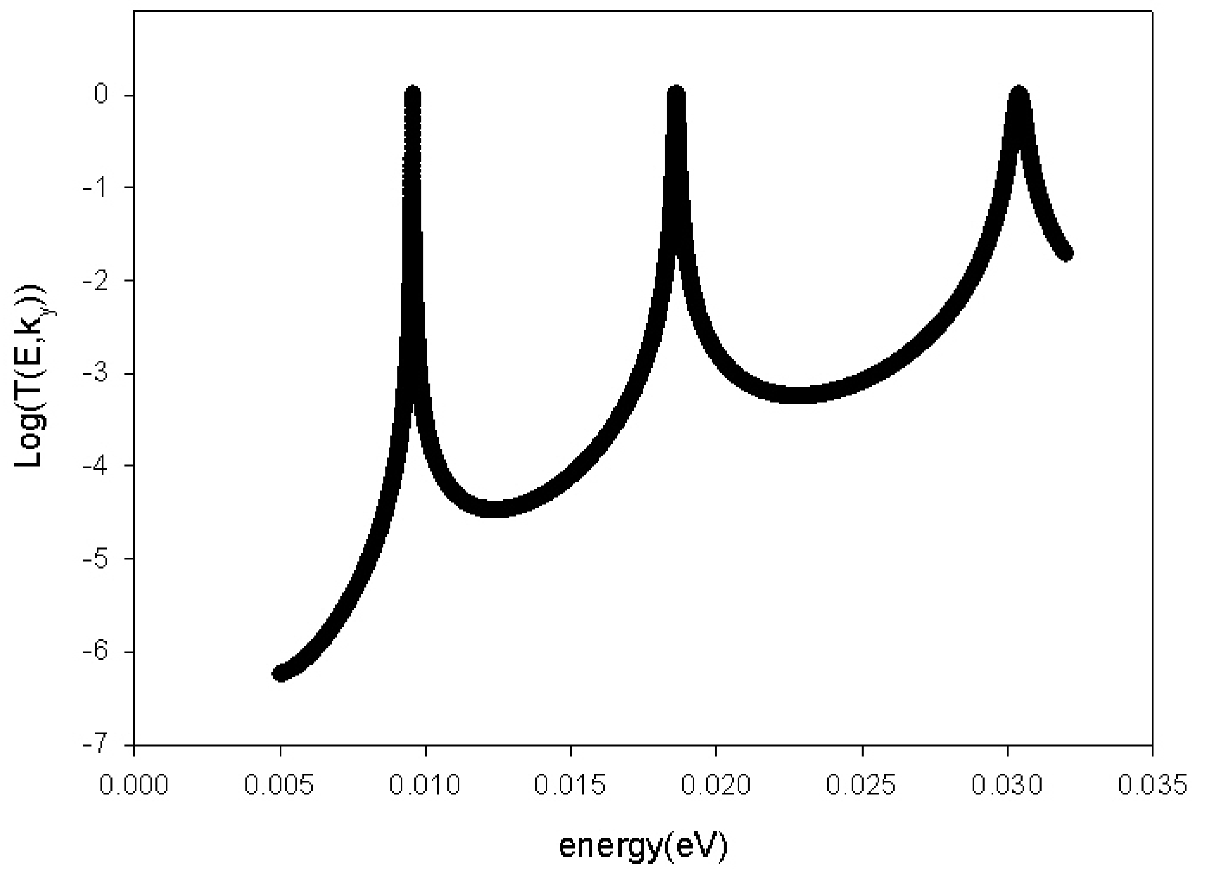

Figure 3.2: Tunneling transmission probability based on logarithm scale is energy dependent. ($k_y = 0.5 \times 10^8\, m^{-1}$)

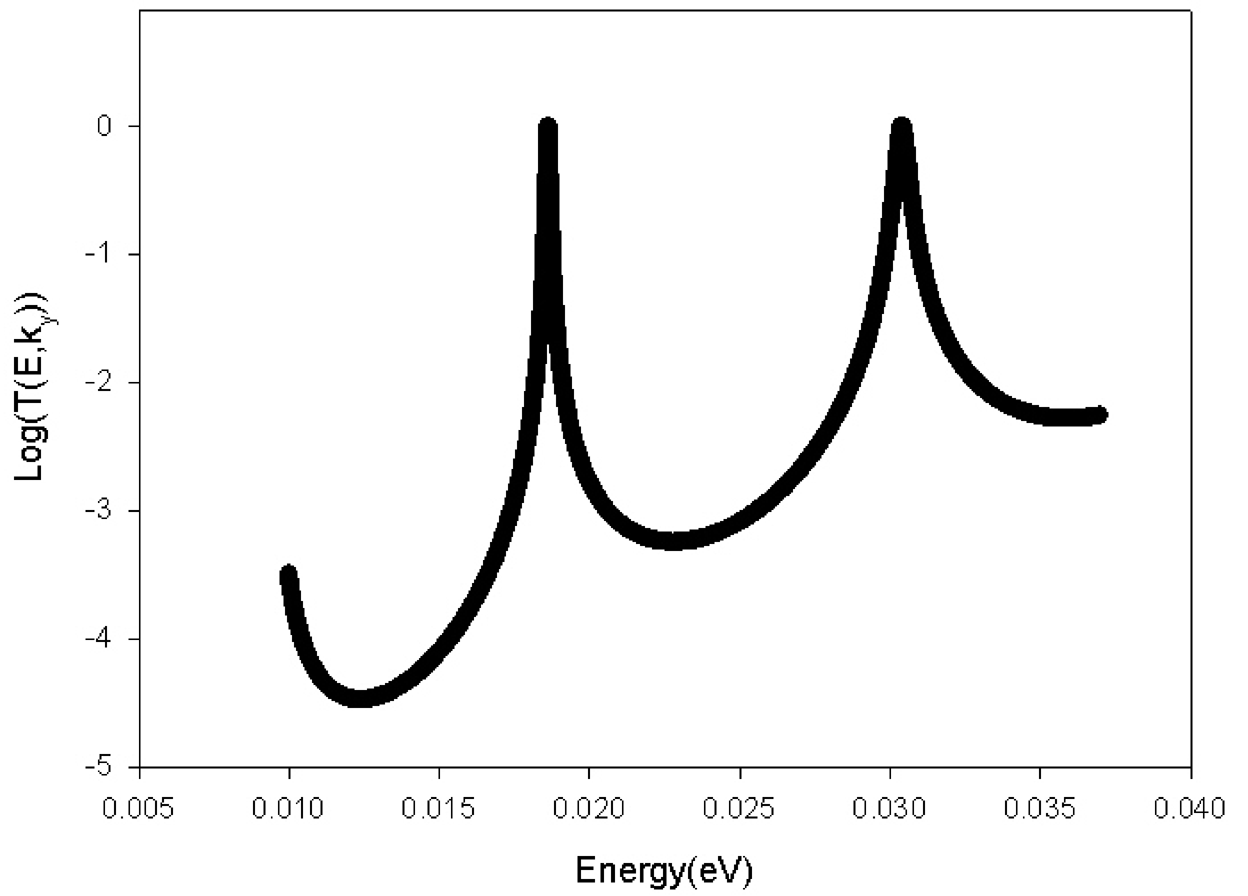

Figure 3.3: Tunneling transmission probability based on logarithm scale depends on electron energy. $(k_y = 1 \times 10^8 \, m^{-1})$.

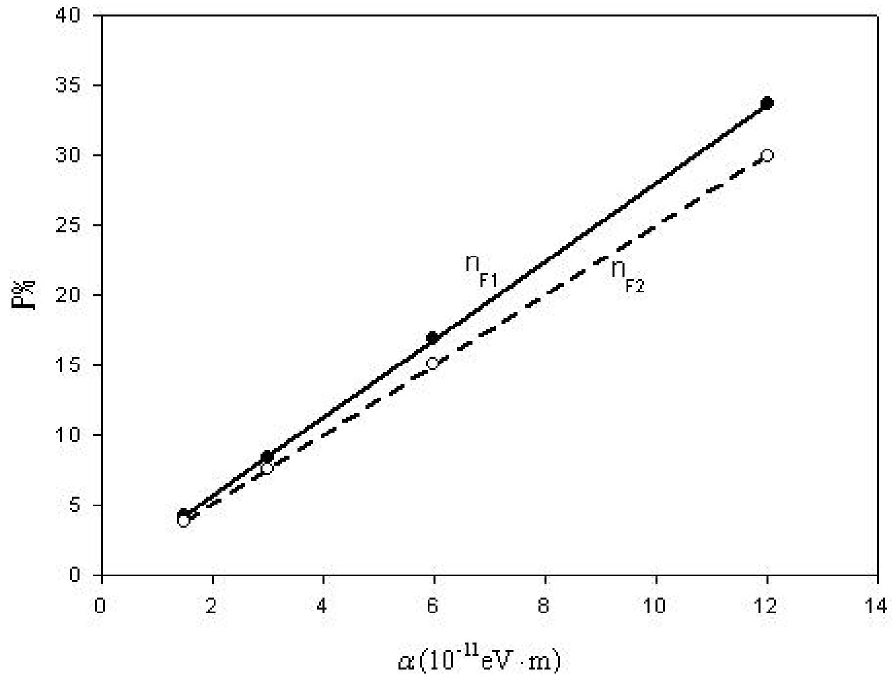

Figure 3.4: Spin polarization depends on spin-orbit interaction parameter linearly at zero temperature and voltage drop($0.00137\,V$) based on the two doping concentrations. ($n_{F1}\ =\ 1.93 \times 10^{11}\ cm^{-2},\ n_{F2}\ =\ 2.42 \times 10^{11} cm^{-2}$)

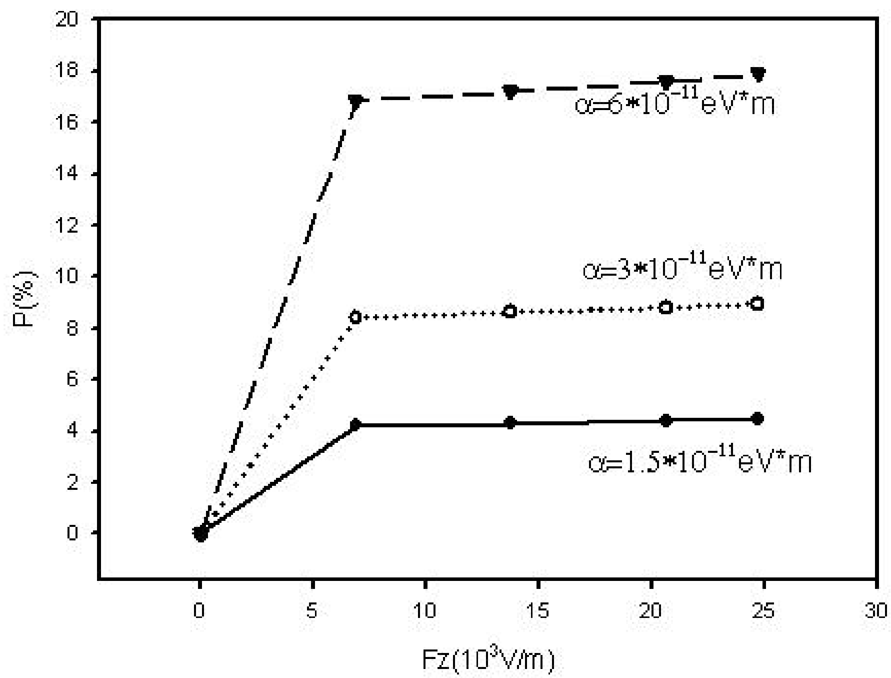

Figure 3.5: Spin polarization is a function of the external electric field, F_z ,under three different spin-orbit interaction parameters.($n_F = 1.93\times 10^{11} cm^{-2}$, $T = 0\,K$)

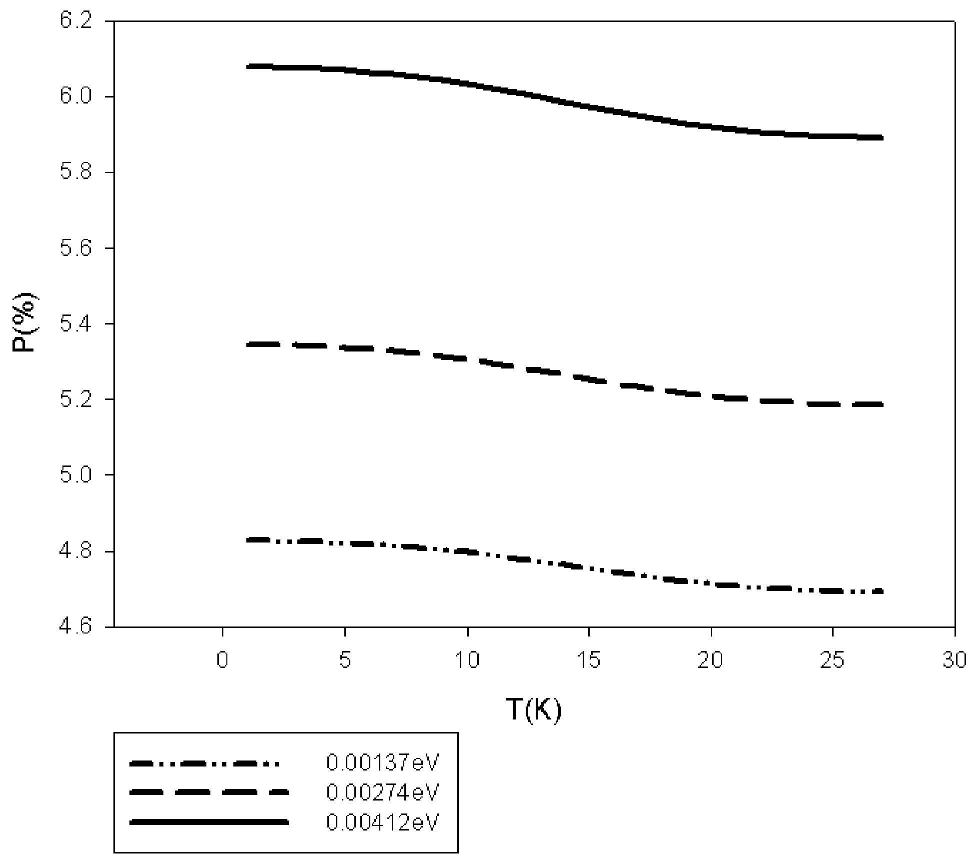

Figure 3.6: Spin polarization depends on temperature based on three different bias values.($n_F = 1.72 \times 10^{11}\, cm^{-2}$, $\alpha = 1.5 \times 10^{-11}\, eV \cdot m$)

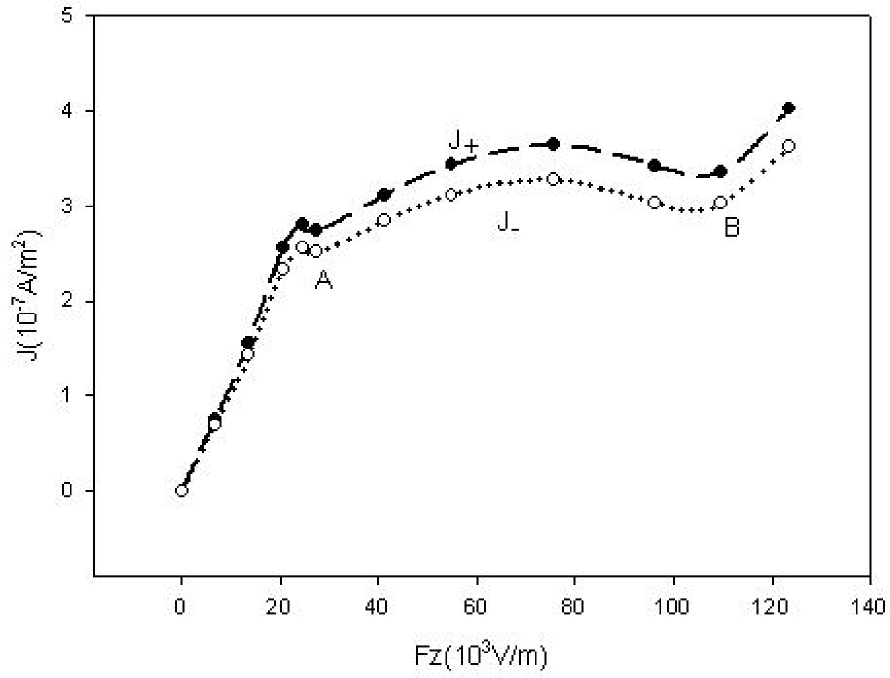

Figure 3.7: J_+ represents spin-up current, and J_- represents spin-down current. And the bias points(A and B) mean the different energy states appear or disappear.($n_F = 1.93 \times 10^{11}\, cm^{-2}$,$\alpha = 1.5 \times 10^{-11}\, eV \cdot m$,$T = 0\, K$)

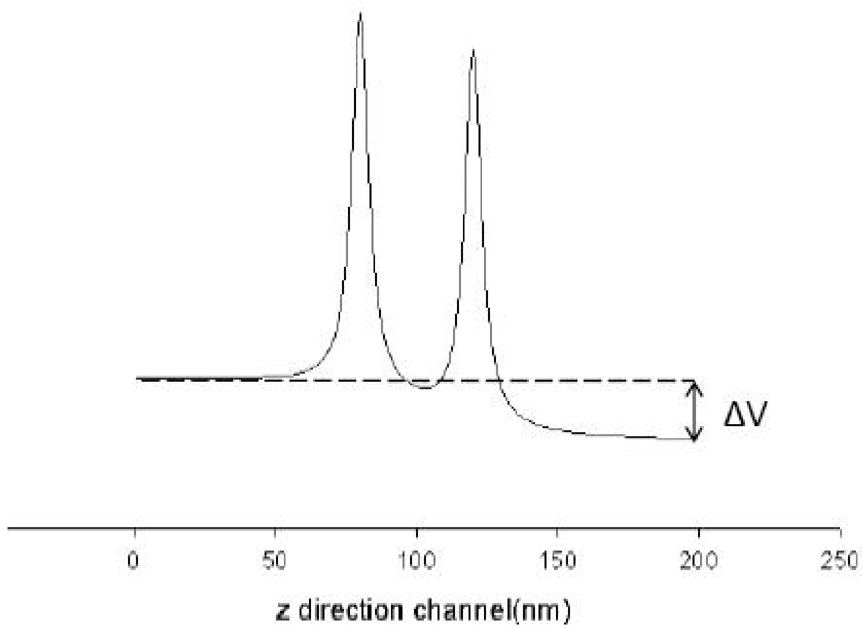

Figure 3.8: The distance between the centers of the double gates is shorten to 40 nm, and ΔV represents the voltage drop.

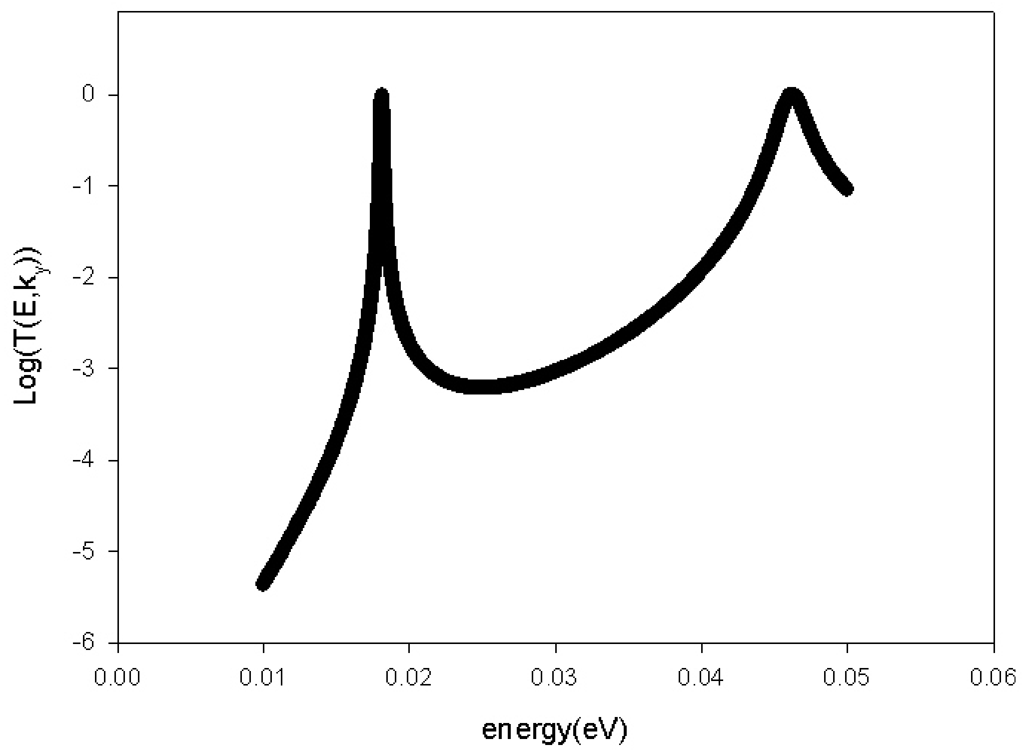

Figure 3.9: The first energy state in the short barrier have been lifted up to 0.018eV.

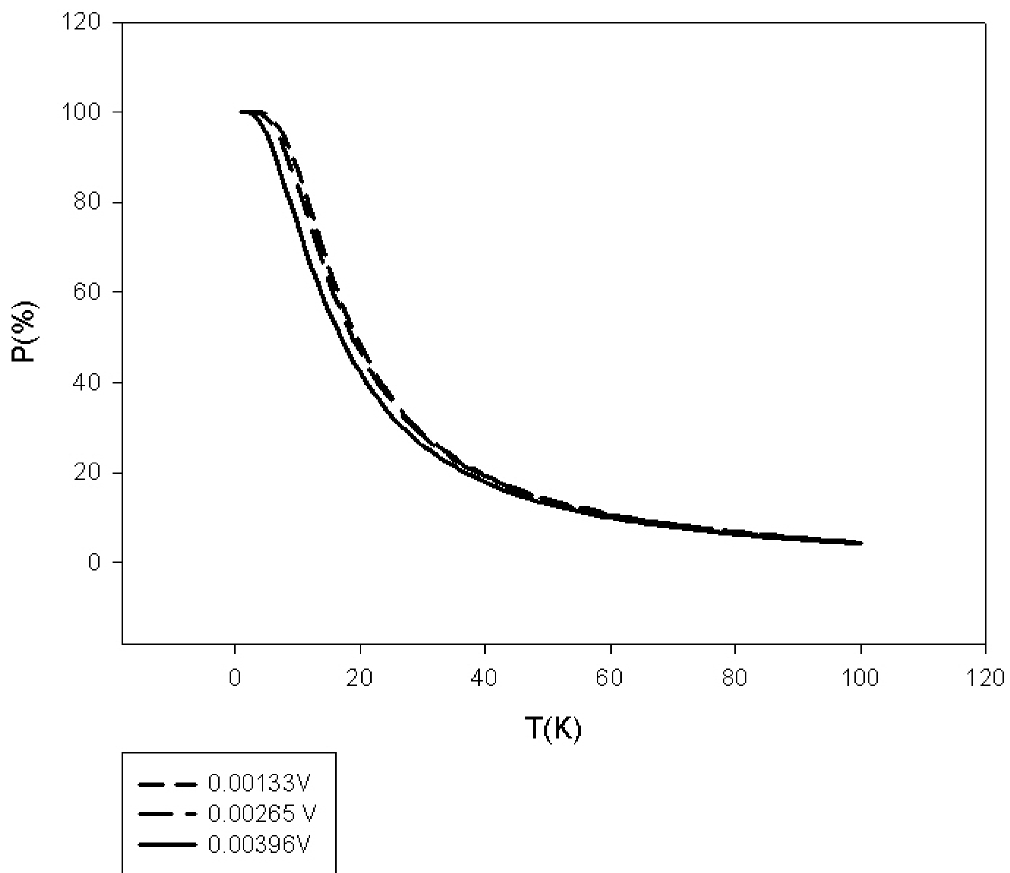

Figure 3.10: Spin polarization remains 100% in a low temperature region and decays fast as the temperature increasing.($n_F = 1.72 \times 10^{11} cm^{-2}$, $\alpha = 1.5 \times 10^{-11}\, eV \cdot m$)

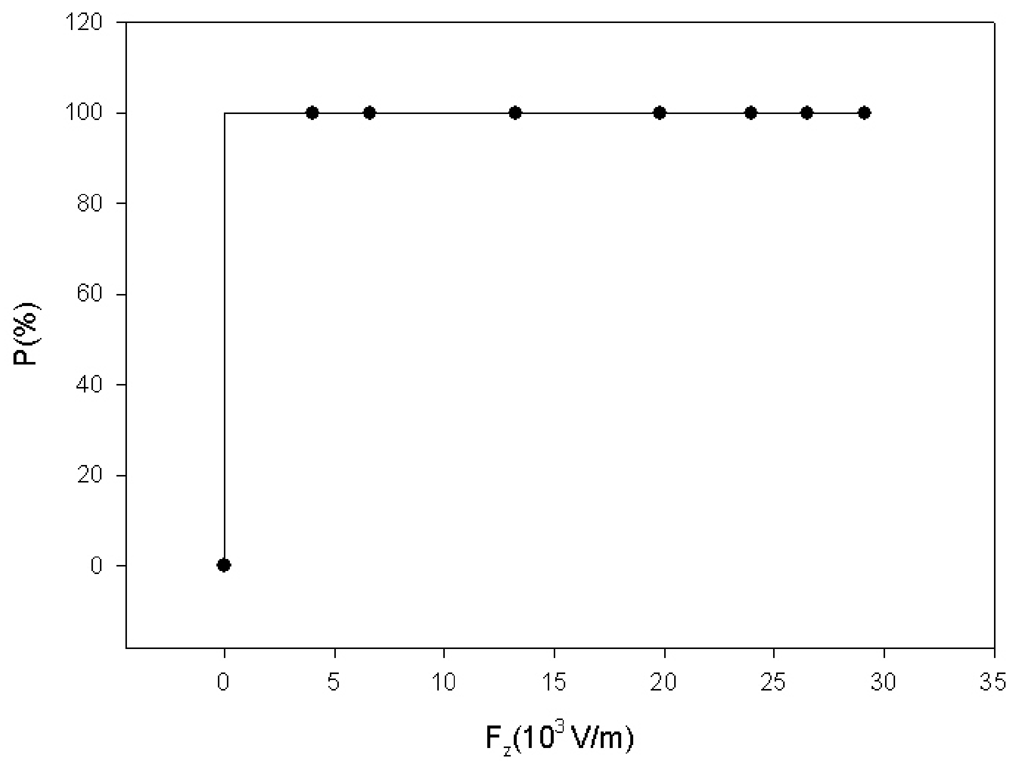

Figure 3.11: 100% polarization remains in a short bias region.($n_F = 1.72 \times 10^{11} cm^{-2}, \alpha = 1.5 \times 10^{-11}\, eV \cdot m, T = 0\, K$)

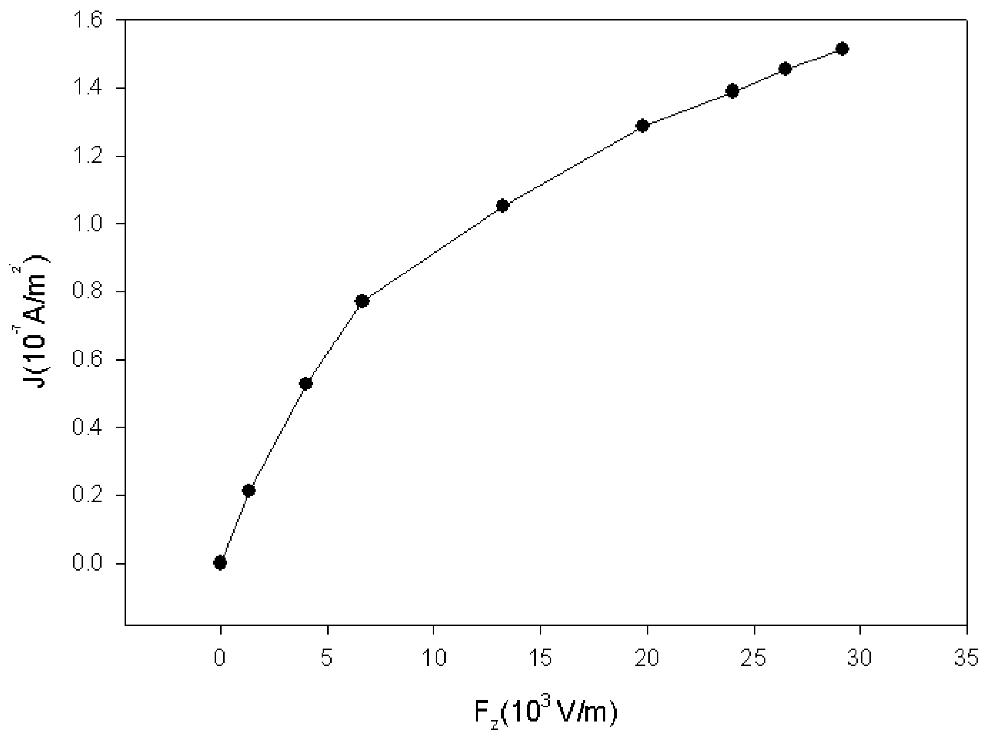

Figure 3.12: The current is only for a spin-down current and nearly linear with the external electric field in the low bias region at zero temperature.($n_F = 1.72 \times 10^{11}\ cm^{-2}$,$\alpha = 1.5 \times 10^{-11}\ eV \cdot m$)

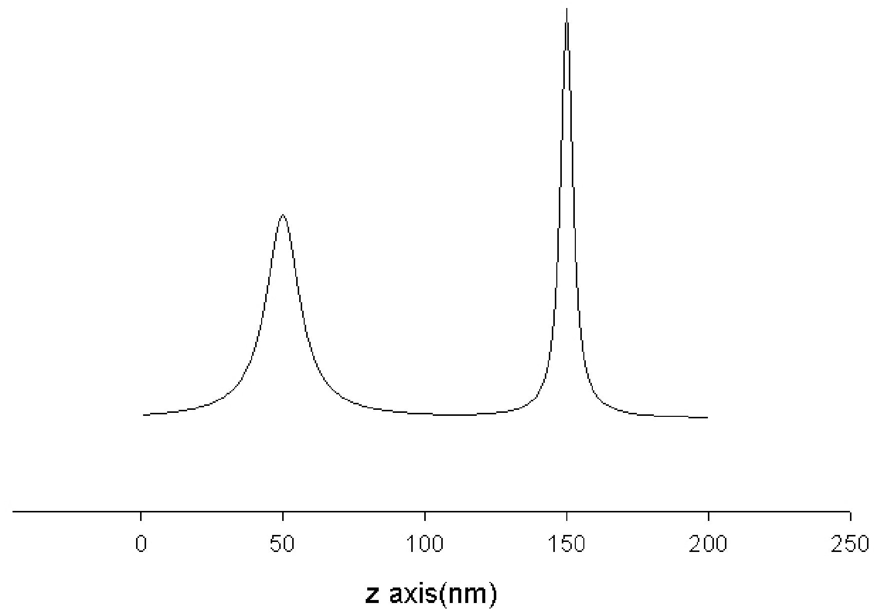

Figure 3.13: The two barriers induced by the mismatch gates along the z axis have different heights(0.1V and 0.2V) and half width(17nm, 9nm).

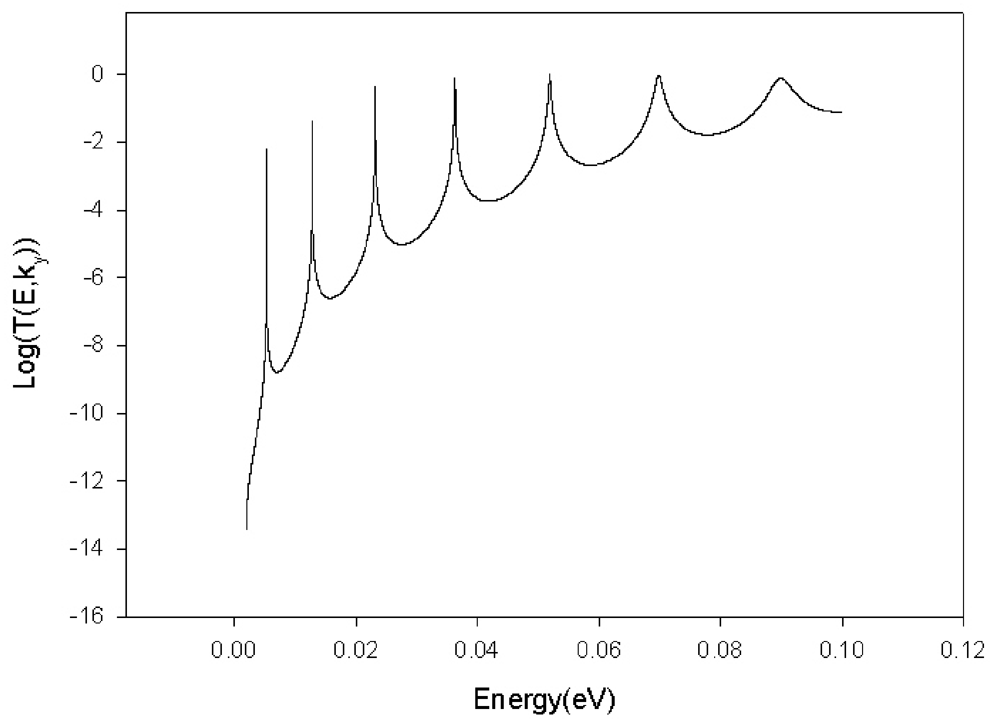

Figure 3.14: The tunneling transmission probability based on logarithm scale is calculated from the asymmetric barrier, and there are still energy states here.

Chapter 4

Conclusions

Research and applications of spin-dependent transport in semiconductor often require spin-polarized electronic current.[18] From this perspective, and active search for new opportunities to obtain spin-polarized current in quantum semiconductor structure is essential. An approach to control the spin-dependent transport in the structures without magnetic field can be a potential advantage and it is worth investigating.

From the work shown in chapter 3, we obtain some details in this gate control potential barrier system. Firstly, the multi-step approximation is feasible to the calculation of this system regardless of the shape of the potential barrier. Then, an electron could penetrate the barrier with a low energy only when the longitudinal energy matches the energy level of the quantum well along the z direction. Rashba term is a key point to the spin polarization especially in this system. And we also get a recognizable magnitude of spin polarization up to 20%. Moreover, with a good control in the doping concentration and the distance between the double gates, we could get 100% spin polarization. It might paves a way for future spin electronic filter. As for the I-V curve, we explain every bias point on the plot. And this idea makes the

spin filer come true.

Moreover, we ensure that this gate control potential system is another way to get a large spin polarization without magnetic field except for the discontinuous parameters for the confined potential in the hetrostructures.

Finally, we want to point out that the calculation presented uses a simple model of a simple effective quasi-one dimensional one-electronic-band Hamiltonian and non-parabolic approximation. The structures have realistic parameters, but the proposed estimate of the total polarized current is only a starting point for the investigations of this new effect. Further experimental investigations of the effect are really needed.

Bibliography

[1] B. Datta and S. Das, Appl. Phys. Lett. **56**, 665 (1990).

[2] R. Tsu and L. Esaki, Appl. Phys. Lett. **22**, 562 (1973).

[3] T. B. Boykin, Phys. Rev. B. **51**, 4289 (1995).

[4] V. V. Paranjape, Phys. Rev. B.**52**, 10 740 (1995).

[5] X. H. Wang, B. Y. Gu, and G. Z. Yang, Phys. Rev. B **55**, 9340 (1997).

[6] S. Bandyyopadhyay, Phys. Rev. B. **61**, 13813(2000)

[7] Y. A. Byshkov and E. I. Rashba, J. Phy. C **17**, 6039(1984)

[8] D. Grundler, Phys. Rev. Lett. **84**, 6074(2000).

[9] J. Nitta, T. Akazaki, and H. Takayanagi, Phys. Rev. Lett. **78**, 1335 (1997).

[10] E. A. de Andrada e Silva, Phys. Rev. B **46**, 1921 (1992); E. A. de Andrada e Silva, and G. C. La Rocca, Phys. Rev. B **50**, 8523 (1994).

[11] A. Voskoboynikov, S.S. Liu, and C.P. Lee, Phys. Rev. B **59**, 12 514 (1999).

[12] E. A. de Andrada e Silva, and G. C. La Rocca, Phys. Rev. B **59**, 15583 (1999).

[13] A. Voskoboynikov, S.S. Liu, and C.P. Lee, J. Appl. Phys. **87**, 387 (2000).

[14] T. Koga, J. Nita, H. Takayanagi, and S. Datta, Phys. Rev. Lett. **88**, 126601 (2002).

[15] Z.-Y. Ting, D. X. Cartoixá, D. H. Chow, J. S. Moon, D. L. Smith, T. C. McGill, and J. N. Schulman, Proc. IEEE, **91**, 741 (2003).

[16] G. Bastard, *Wave Mechanics Applied to Semiconductor Heterostructures* (Les Edition de Physique, Les Ulis, 1990).

[17] Yuji Ando, and Tomohiro Itoh, J. Appl. Phys.**61**, 4 (1987).

[18] P. Bruno and J. Wunderlich, J. Appl. Phys. **84**, 978 (1998).

[19] S. G. Shen and X. Q. Fan, J. Phys.: Condens. Matter **9**, 3151 (1997).

[20] G. Schmidt, D. Ferrand, L.W. Molenkamp, A.T. Filip,and J. van Wees, Phys. Rev. B **62**, R4970 (2000).

[21] G. Dresselhaus, Phys. Rev. **100**, 580 (1955).

[22] V. I. Perel', S. A. Tarasenko, I. N. Yassievich, S. D. Ganichev, V. V. Bel'kov, and W. Prettl, Phys. Rev. B **67**, 201304 (2003).

[23] E. O. Kane, *Tunneling Phenomenon in Solids* (Plenum, New York, 1969).